Journal of Pain Research

Dovepress
Taylor & Francis Group

Open Access Full Text Article

ORIGINAL RESEARCH

Identification of Pyroptosis-Related Genes in Male Rats with Spared Nerve Injury-Induced Neuropathic Pain

Wangyu Li[1,2,*], Zhouting Hu[3,*], Peng Lin[1,2,*], Long He[1,2], Rongguo Liu[1,2]

[1]Department of Painology, the First Affiliated Hospital of Fujian Medical University, Fuzhou, Fujian, People's Republic of China; [2]Department of Painology, National Regional Medical Center, Binhai Campus of the First Affiliated Hospital of Fujian Medical University, Fuzhou, Fujian, People's Republic of China; [3]Department of Anesthesiology, Hospital of Chengdu University of Traditional Chinese Medicine, Chengdu, Sichuan, People's Republic of China

*These authors contributed equally to this work

Correspondence: Long He; Rongguo Liu, Email 1038370096@qq.com; 9201151029@fjmu.edu.cn

Purpose: Pyroptosis, a programmed inflammatory cell death mechanism, plays a significant role in neuropathic pain (NP) pathogenesis. However, the specific pyroptosis-related genes (PRGs) driving NP development remain poorly understood. This study employs systematic approaches to identify and validate PRGs, aiming to delineate their mechanistic contributions to NP progression.

Methods: To elucidate pyroptosis-related genes (PRGs) in neuropathic pain pathogenesis, we first performed integrated bioinformatics analysis of the GSE236754 dataset, revealing differentially expressed PRGs in the spinal cord dorsal horn of spared nerve injury (SNI) rats. Subsequent functional enrichment analyses coupled with protein-protein interaction network construction delineated pathway convergences among identified PRGs. Experimental validation utilizing SNI rat model, Western blot and immunofluorescence quantification confirmed protein expression patterns, and immunofluorescence mapping determined cellular localization collectively. Statistical analyses via ANOVA method.

Results: Bioinformatics screening identified 11 candidate PRGs in the SNI model, particularly highlighting Nlrc4 and Nlrp3 as the most upregulated targets. Gene Ontology (GO) analysis demonstrated significant enrichment in three domains, pyroptosis regulation, inflammasome complex assembly, and cysteine-type endopeptidase activity associated. Kyoto Encyclopedia of Genes and Genomes (KEGG) pathway analysis specifically identified the "NOD-like receptor signaling pathway" as significantly enriched. Gene Set Enrichment Analysis (GSEA) further corroborated these findings. Behavioral quantification showed progressive mechanical hypersensitivity, with mechanical pain and cold pain reaching maximal sensitivity at day 7 post-injury ($p<0.001$). Western blot detected synchronized elevation of NLRP3 and NLRC4 inflammasome components and downstream effectors across the observation window (all $p<0.05$). Immunofluorescence analysis demonstrated a time-dependent increase in the expression of GSDMD-N, the pyroptotic-executing protein, a trend consistent with the findings from behavioral tests and Western blot analysis ($p<0.05$). And cellular localization analysis revealed neuron-predominant accumulation of GSDMD-N.

Conclusion: We identified 11 potential biomarkers for NP. Our data conclusively show that SNI induced NLRP3/NLRC4 inflammasome activation and neuronal pyroptosis in the rat spinal cord.

Keywords: neuropathic pain, pyroptosis, bioinformatics, causal relationship, inflammasome

Introduction

Neuropathic pain (NP), operationally defined per the International Association for the Study of Pain (IASP) guidelines as somatosensory system pathology-induced pain,[1] is etiologically stratified into peripheral and central subtypes. The condition's recent inclusion in ICD-11 as a distinct diagnostic category[2] reflects its clinical significance, given the 3–17% population prevalence and characteristic chronic trajectory marked by refractory pain cycles that severely compromise quality of life and healthcare resources.[3] Over 50% of patients report inadequate pain relief from existing

Received: 10 October 2025
Accepted: 17 December 2025
Published: 23 December 2025

medications underscore the urgent need to decipher NP's complex pathobiology, now recognized as a premier translational neuroscience challenge.[4]

The immune-neural axis plays a pivotal role in NP pathophysiology, where dysregulated inflammatory cascades in both peripheral and central nervous systems drive pain initiation and chronicity.[5–7] A hallmark of NP involves spinal dorsal horn nociceptive neuron hyperexcitability (central sensitization), concomitant with cytokine-mediated neuroinflammatory amplification mechanisms.[8] Pyroptosis is a lytic programmed cell death modality that features progressive cell swelling culminating in plasma membrane rupture and pro-inflammatory mediator release.[9] Canonical pyroptotic signaling proceeds through sequential stages: NLR sensor activation, Caspase-1-mediated GSDMD cleavage then plasma membrane nanopore formation. These molecular events orchestrate IL-1β/IL-18 secretion cascades that simultaneously execute cell death and instigate tissue-level inflammation.[10,11] Emerging preclinical evidence substantiates pyroptosis inhibition as a viable anti-neuroinflammatory strategy across multiple NP models, with corresponding pain attenuation.[12] These findings collectively position pyroptotic pathway modulation as a promising therapeutic frontier, necessitating deeper mechanistic dissection. However, research into the relationship between NP and pyroptosis has predominantly focused on the NLRP3 inflammasome and Chronic Constriction Injury (CCI) model. This study aims to identify other potential pyroptosis-related genes(PRGs) that may be involved in Spared Nerve Injury (SNI) rat.

In this study, we aimed to identify PRGs as potential biomarkers by analyzing whole transcriptome RNA-seq data from spinal cord samples from SNI and sham groups of Rattus norvegicus. And, Western blot validation of pyroptotic effector proteins in SNI model spinal cord lysates and dual immunofluorescence colocalization identification cellular specificity of pyroptotic events was mapped.

Materials and Methods

Ethics Statement

All experimental protocols were reviewed and approved by the Experimental Animal Welfare Ethics Committee of Fujian Medical University (IACUC FJMU-2024-Y-2455). This study was conducted in strict accordance with the recommendations of the NIH's Health Guide for the Care and Use of Laboratory Animals. All procedures were performed under sodium pentobarbital anesthesia, and efforts were made to minimize distress. This study exempt from approval based on item 1 and 2 of Article 32 of the Measures for Ethical Review of Life Science and Medical Research Involving Human Subjects dated February 18, 2023, China. Following the experimental procedures, euthanasia was performed by administering a lethal dose of sodium pentobarbital intraperitoneally.

Data Collection and Processing

Transcriptomic profiles (GSE236754 dataset) were retrieved from NCBI's Gene Expression Omnibus (GEO),[13] generated via Illumina HiSeq 4000 sequencing (GPL22396 platform). This study analyzed transcriptomic data from ipsilateral spinal cord dorsal horn tissues of male rats collected 7 days post-surgery, comparing SNI and Sham groups, with 4 biological replicates per group (SNI: n=4; Sham: n=4). Raw sequencing data underwent quality control using fastp (version 0.22.0) with default parameters. The reference genome mRatBN7.2, sourced from the National Center for Biotechnology Information (NCBI) repository (Accession No. GCF_015227675.2), represents a significant update since the Rnor6.0 release by the Rat Genome Sequencing Consortium in 2014, offering improved gene annotation completeness.[14,15] HISAT2 v2.2.1-indexed genome mappings were converted to BAM format via Samtools v1.17, with transcript abundance quantified using featureCounts v2.0.1. PRGs were systematically curated by integrating multiple resources: (1) literature mining from peer-reviewed publications,[16] (2) Gene Ontology Biological Processes Annotation (http://geneontology.org/),[17] and (3) the Molecular Signatures Database (MSigDB, v2023.2).[18] Species-specific gene name conversion (eg, mouse to rat) was achieved using the bioMart tool suite.

Screening of Differentially Expressed PRGs

Bioinformatic analyses were executed in R v4.3.2 and NetworkAnalyst (https://www.networkanalyst.ca/).[19] Initial dimensionality reduction through principal component analysis (PCA) assessed dataset quality control. Differential

expression profiling was subsequently performed with DESeq2 (v1.40.2), p-value <0.05 and absolute log2-transformed fold change (|log2FC|) >0.5 as significance thresholds. PRGs candidates were identified through intersection analysis of differentially expressed genes (DEGs) with pre-curated PRG libraries. Visualization pipelines implemented in ggplot2 generated Venn diagrams, clustered heatmaps, and annotated volcano plots.

Functional Enrichment Analysis of Differentially Expressed PRGs

The clusterProfiler package implemented three complementary enrichment strategies: (a) Gene Ontology (GO) functional categorization across biological processes (BP), cellular components (CC), and molecular functions (MF) domains; (b) Kyoto Encyclopedia of Genes and Genomes (KEGG) pathway mapping; and (c) Gene Set Enrichment Analysis (GSEA).[20] Whereas GO and KEGG interrogate individual gene significance, GSEA evaluates coordinated expression patterns across predefined gene sets, enhancing detection of subtle but biologically coherent signals.[21] All analyses employed the org.Rn.eg.db annotation database (v3.16.0) with false discovery rate (FDR) correction (Benjamini-Hochberg method).

Protein Interactome Profiling of DEPRGs

The STRING online database (https://string-db.org/)[22] was used to construct PPI networks, exploring potential interactions among proteins related to the focal process. PPI networks were visualized using Cytoscape (version 3.9.1), and hub genes were identified using the MCC method in the CytoHubba plugin. Additionally, correlation analysis was performed using the Spearman package in R.

Animal and SNI Model

Male Sprague-Dawley rats (body weight 250–300 g) were sourced from the accredited Animal Center of Fujian Medical University. Following ≥7-day acclimatization under specific pathogen-free conditions, SNI modeling was conducted.[23] In brief, rats received intraperitoneal anesthesia with sodium pentobarbital (50 mg/kg; 1% w/v solution). Through a lateral mid-thigh incision, the left sciatic trifurcation was exposed. Both tibial and common peroneal nerves underwent double ligation (5–0 silk) followed by 3-mm segment excision, preserving the sural nerve. Surgical closure involved sequential muscle layer (4–0 vicryl) and skin (3–0 nylon) suturing. Sham controls underwent identical exposure without neural manipulation.

Paw Mechanical Withdrawal Threshold (PMWT)

Mechanical allodynia was assessed using the Dixon up-down paradigm.[24] Preoperatively and at postoperative days 3, 7, and 14, Von Frey filaments (Stoelting Co., USA; 0.008–300g force range) were applied perpendicularly to the plantar surface of ipsilateral hindpaws. Rats underwent 30-min acclimation in standardized plexiglass enclosures (30×30×40 cm) prior to testing. Starting with 4.0g filament (5.18 bending force), mechanical stimuli were delivered through the mesh floor (4 mm^2 contact area) for exactly 3 seconds. Positive nocifensive responses (rapid paw withdrawal, licking, or shaking) triggered filament force reduction, whereas negative responses prompted force escalation.

Acetone Test

After the Von Frey test, cold pain behavior was assessed by applying acetone (100 μL) to the plantar surface of the hind paw using an insulin needle. Responses to acetone application were observed for 1 minute, and pain scores were graded as follows: 0, no response; 1, rapid paw retraction or flicking; 2, prolonged withdrawal or flicking; and 3, repeated flicking and licking. Acetone was applied to each hind paw 3 times (every 5 min) and averaged.

Experimental Materials Preparation

Under deep anesthesia (sodium pentobarbital 50 mg/kg i.p.; 1% w/v solution), experimental animals underwent terminal procedures. For Western blot analysis, spinal cord tissues (approximately 1.5 cm segments from lumbar segments L4-L6) were rapidly isolated via laminectomy. The collected segments were then bisected longitudinally along the anterior median fissure. The ipsilateral side of the spinal cord was promptly frozen in liquid nitrogen-cooled isopentane and

stored in cryovials (Thermo Scientific) at −80°C. For immunofluorescence, animals were transcardially perfused. The perfusion was initiated with ice-cold phosphate-buffered saline (PBS), followed by 500 mL of ice-cold 4% paraformaldehyde (PFA). Successful perfusion was confirmed by observable rigidity of the limbs and neck, as well as blanching of the liver. The spinal column was then dissected, and the lumbar enlargement of the spinal cord was carefully removed. The tissue was post-fixed in 4% PFA at 4°C for 24 hours and subsequently cryoprotected in a 30% sucrose solution until it sank to the bottom of the container. Upon sucrose infiltration, the tissue was embedded in OCT compound and sectioned at a thickness of 15 μm using a cryostat. The resulting sections were stored at −20°C.

Western Blot

Lumbar spinal cord tissues were homogenized in ice-cold RIPA buffer (Servicebio G2002; 50 mM Tris-HCl pH 7.4, 150 mM NaCl, 1% NP-40, 0.5% sodium deoxycholate) using a Polytron PT 1200E homogenizer (3×10 s pulses at 15,000 rpm). Lysates were centrifuged at 12,000×g (4°C, 10 min) and supernatants quantified via BCA assay (G2026, Servicebio). Protein samples (30 μg) were resolved on 10% Bis-Tris gels (Invitrogen) under reducing conditions and transferred to 0.45 μm PVDF membranes (Millipore) using Towbin buffer (25 mM Tris, 192 mM glycine) at 100 V for 90 min. Following a 2-hour block with 5% skim milk at room temperature, the membranes were incubated overnight at 4°C with the indicated primary antibodies. Antibodies applied included those against NLRP3 (A5652, Abclonal), NLRC4 (A24336, Abclonal), ASC (A22046, Abclonal), Cleaved-Caspase-1 (AF4005, Affinity), the pyroptosis-executor GSDMD-N (A22523, Abclonal), IL-1β (A1112, Abclonal), IL-18 (10,663-1-AP, Proteintech), and GAPDH (GB11002-100, Servicebio) as a loading control, all diluted according to the manufacturers' specifications. After 3×10 min TBST washes, membranes were incubated with HRP-conjugated goat anti-rabbit IgG (ab205718, Abcam) for 2 h at 22°C. Chemiluminescent signals were developed with ECL Prime (G2161, Servicebio) and captured using Image Lab 6.1 (Bio-Rad). Band intensities were quantified via rolling ball background subtraction (radius 50 pixels) in ImageJ 1.53t (NIH).

Immunofluorescence

Following antigen retrieval, tissue sections underwent three 5-minute phosphate-buffered saline (PBS) washes. Non-specific binding was blocked using 5% bovine serum albumin (BSA; Sigma) for 1 h at room temperature (RT). Primary antibodies were then applied and incubated at 4°C overnight, including: GSDMD-N (1:200; Affinity, DF13758), NeuN (1:3000; Abcam, ab177487), GFAP (1:2000; Abcam, ab7260), and Iba1 (1:2000; Abcam, ab178846). After PBS washing, sections were incubated with Horseradish Peroxidase (HRP)-conjugated goat anti-rabbit IgG secondary antibody (1:2000; Abcam, ab205718) at RT for 1 h. Tyramide signal amplification was performed using either Try-488 (1:2000; Runlong Biotechnology, Bry-Try488) or Try-Cy3 (1:2000; Runlong Biotechnology, Bry-TryCy3) under light-protected conditions for 30 min at RT. Nuclei were counterstained with DAPI-containing anti-fade mounting medium (Beyotime, P0131). Imaging was conducted using a Leica DMi8 fluorescence microscope. Quantitative analysis was performed by measuring the mean fluorescence intensity in the ipsilateral dorsal horn of the spinal cord.

Statistical Analyses

Statistical analyses were performed using SPSS 26.0 (IBM Corp.) with visualization created in GraphPad Prism 8.0.2. Continuous data are expressed as mean ± SEM. Paw withdrawal mechanical threshold (PWMT) trajectories were evaluated via two-way repeated measures ANOVA with Geisser-Greenhouse correction. Intergroup differences were determined using Bonferroni-adjusted post hoc tests when significant interaction effects emerged. Protein expression quantifications were compared across groups using one-way ANOVA followed by Bonferroni-corrected pairwise comparisons versus sham controls. All hypothesis testing maintained a pre-specified family-wise error rate at $\alpha = 0.05$ (two-tailed).

Results

Identification of Differentially Expressed PRGs in NP

PCA revealed strong inter-replicate consistency across biological replicates (n=4 per group), with clear spatial segregation between the SNI and sham-operated groups. Differential expression analysis of 70 PRGs identified 11 significantly

upregulated genes, with NLR family members demonstrating the most substantial transcriptional changes. Notably, Nlrc4 and Nlrp3 exhibited the highest fold-changes among DEGs, suggesting their potential role in neuroinflammatory signaling pathways (Figure 1).

GO, KEGG and GSEA Enrichment Analysis

GO analysis demonstrated significant enrichment in three domains: (a) pyroptosis regulation within BP; (b) inflammasome complex assembly in CC; and (c) cysteine-type endopeptidase activity associated in MF. KEGG pathway analysis specifically identified the "NOD-like receptor signaling pathway" as significantly enriched. GSEA further corroborated these findings, showing prominent enrichment in pyroptosis-related NOD-like receptor signaling pathways (Figure 2).

PPI Network Construction and Correlation Analysis

PPI network analysis revealed robust interconnectivity among the identified genes, with Casp1 identified as a central hub gene. Furthermore, correlation analysis demonstrated significant positive correlations across all 11 pyroptosis-related DEGs (Figure 3).

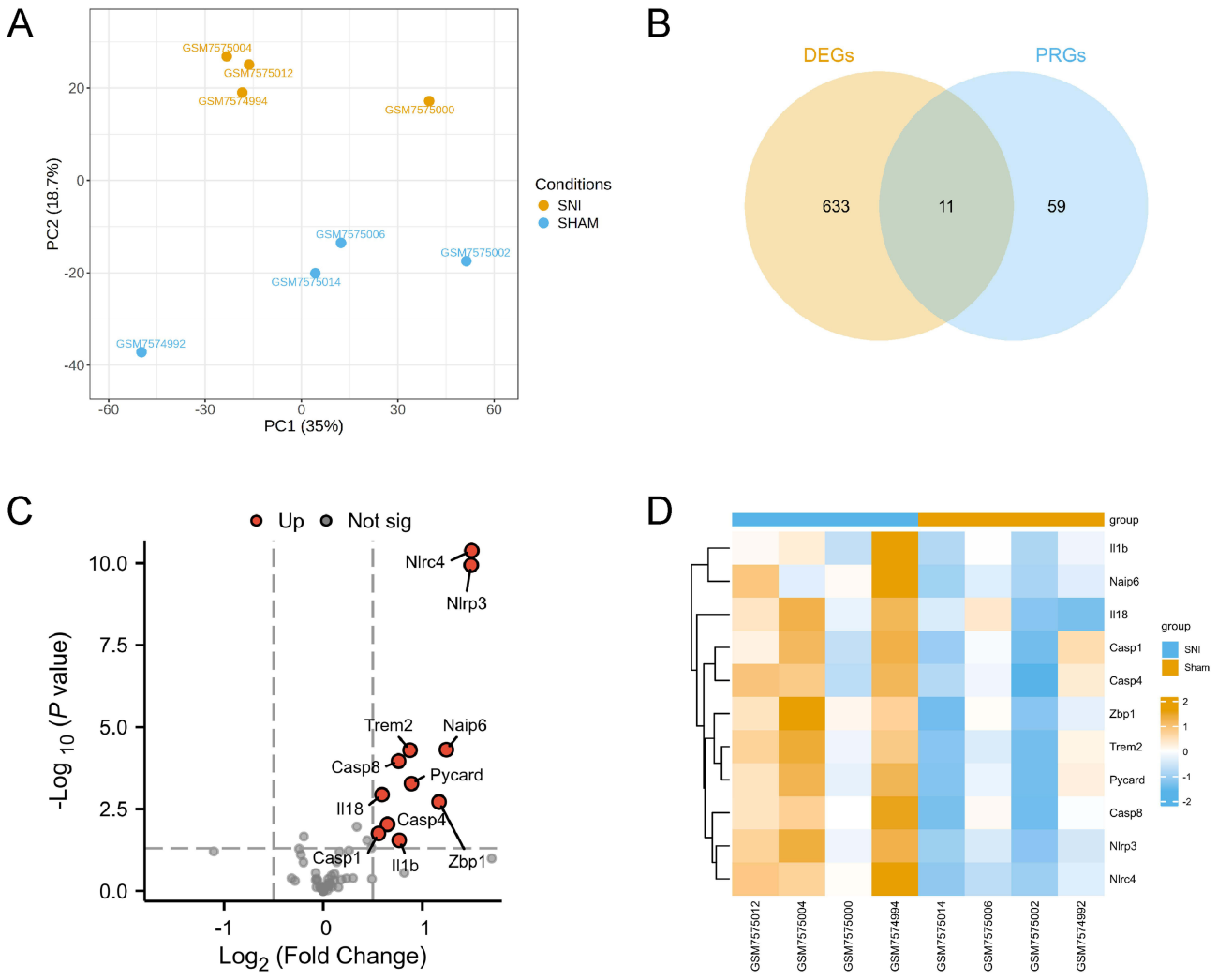

Figure 1 Identification of differentially expressed pyroptosis-related genes in NP. (**A**) PCA of the GSE236754 dataset; (**B**) Venn diagrams show 11 potential key PRGs to be validated; (**C**) Volcano plot of the PRGs. The significantly upregulated genes are represented by red dots; (**D**) Heatmap of the differentially expressed PRGs between the SNI and Sham rat. Pyroptosis-related genes (PRGs), differentially expressed genes (DEGs).

https://doi.org/10.2147/JPR.S568630

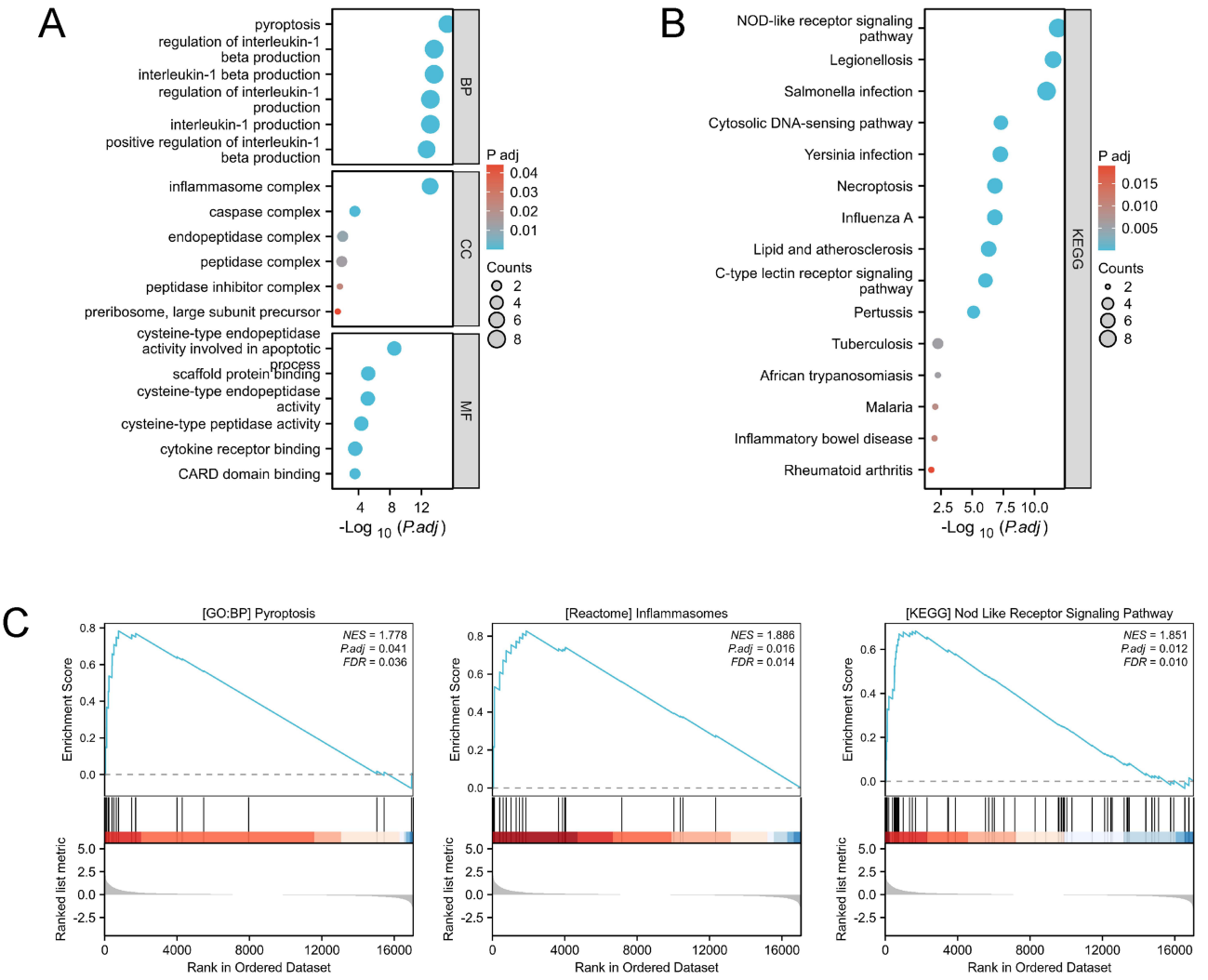

Figure 2 GO, KEGG, and GSEA Enrichment Analysis. (**A**) GO enrichment analysis of the differentially expressed PRGs between the SNI and Sham rat; (**B**) KEGG pathway enrichment analysis; (**C**) GSEA enrichment analysis. Biological processes (BP), cellular components (CC), and molecular functions (MF).

SNI Induces Mechanical Allodynia and NLRP3/NLRC4 Inflammasomes Activation

PMWT was significantly reduced in SNI rats compared to the Sham group, reaching its lowest point on day 7 and persisting until day 14. Cold Allodynia also increases with molding time. Given the significant upregulation of Nlrp3 and Nlrc4, we quantified protein expression levels of NLRP3, NLRC4, and their downstream components-including ASC, caspase-1, GSDMD-N, IL-1β, and IL-18 — in the spinal cord dorsal horn. Immunoblotting demonstrated that NLRP3 and NLRC4 expression progressively increased post-SNI, peaking at postoperative day (POD) 7 with sustained elevation through POD14 ($p<0.001$ vs sham). Parallel temporal patterns increased were observed for ASC, cleaved caspase-1, GSDMD-N, mature IL-1β, and IL-18 (all $p<0.05$) (Figure 4).

SNI Induces Neuronal Pyroptosis

Immunofluorescence analysis demonstrated a time-dependent increase in the expression of GSDMD-N, the pyroptotic-executing protein, a trend consistent with the findings from behavioral tests and Western blot analysis ($p<0.05$). To investigate the cellular mechanisms underlying pyroptosis, immunofluorescence staining was performed to assess the co-localization of GSDMD-N with microglia (Iba-1), astrocytes (GFAP), and neurons (NeuN). Results revealed that GSDMD-N co-localized exclusively with NeuN in the spinal cord dorsal horn, but not with Iba-1 or GFAP (Figure 5).

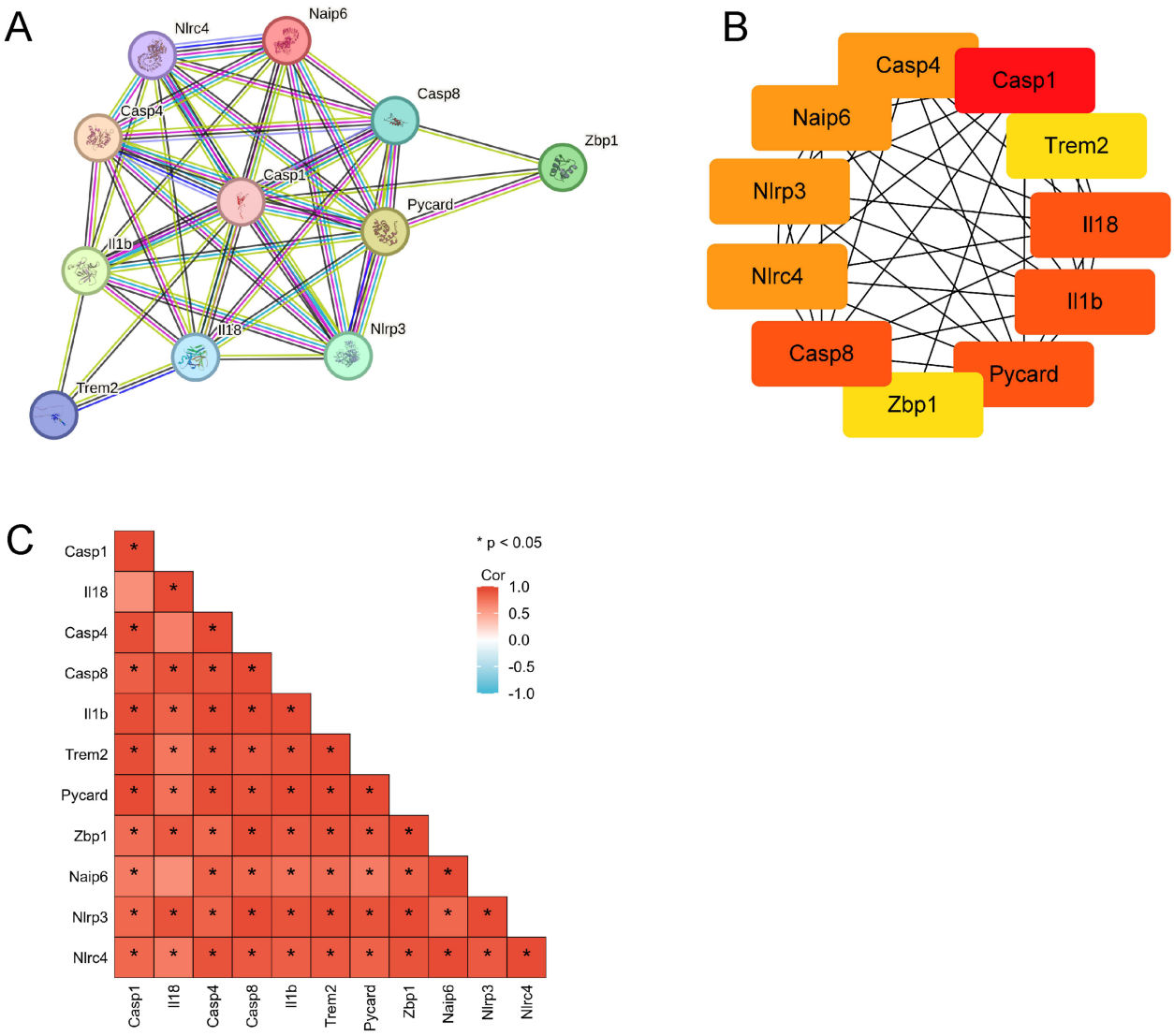

Figure 3 PPI Network Construction and Correlation Analysis. (**A**) PPI network is established by the STRING website; (**B**) Relationship network diagram of PRGs from PPI network using cytoscape; (**C**) Spearman correlation analysis of the 11 differentially expressed PRGs. *p < 0.05. Correlation coefficient (cor).

Discussion

This study identified PRGs in the spinal dorsal horn of rat models of NP through bioinformatics analysis. We found that 11 PRGs are associated with an increased risk of NP. Our data conclusively show that SNI induced NLRP3/NLRC4 inflammasome activation and neuronal pyroptosis in the rat spinal cord.

NP is a prevalent and challenging condition that encompasses PHN, diabetic peripheral neuropathy, and complex regional pain syndrome, among others.[25,26] This type of pain is typically chronic, substantially affecting patients' physical and mental health,[27] resulting in elevated disability rates, poor treatment outcomes, and higher economic burdens.[28] Current evidence suggests that neuroinflammation plays a critical role in the development and progression of NP.[8] Pyroptosis, a novel form of inflammatory cell death characterized by cell membrane rupture and the release of inflammatory cytokines, has been identified as a potential contributor to NP. Investigating the role of pyroptosis in NP pathogenesis may provide novel avenues for the treatment and prevention of NP.

We discovered 11 PRGs (Nlrp3, Pycard, Zbp1, Il18, Il1b, Casp8, Nlrc4, Casp1, Casp4, Naip6, and Trem2) associated with NP. The classical pyroptosis pathway is characterized by the activation of caspase-1 by the inflammasome, which subsequently cleaves GSDMD, resulting in cell pyroptosis and the subsequent cleavage and release of IL-1β and IL-

https://doi.org/10.2147/JPR.S568630

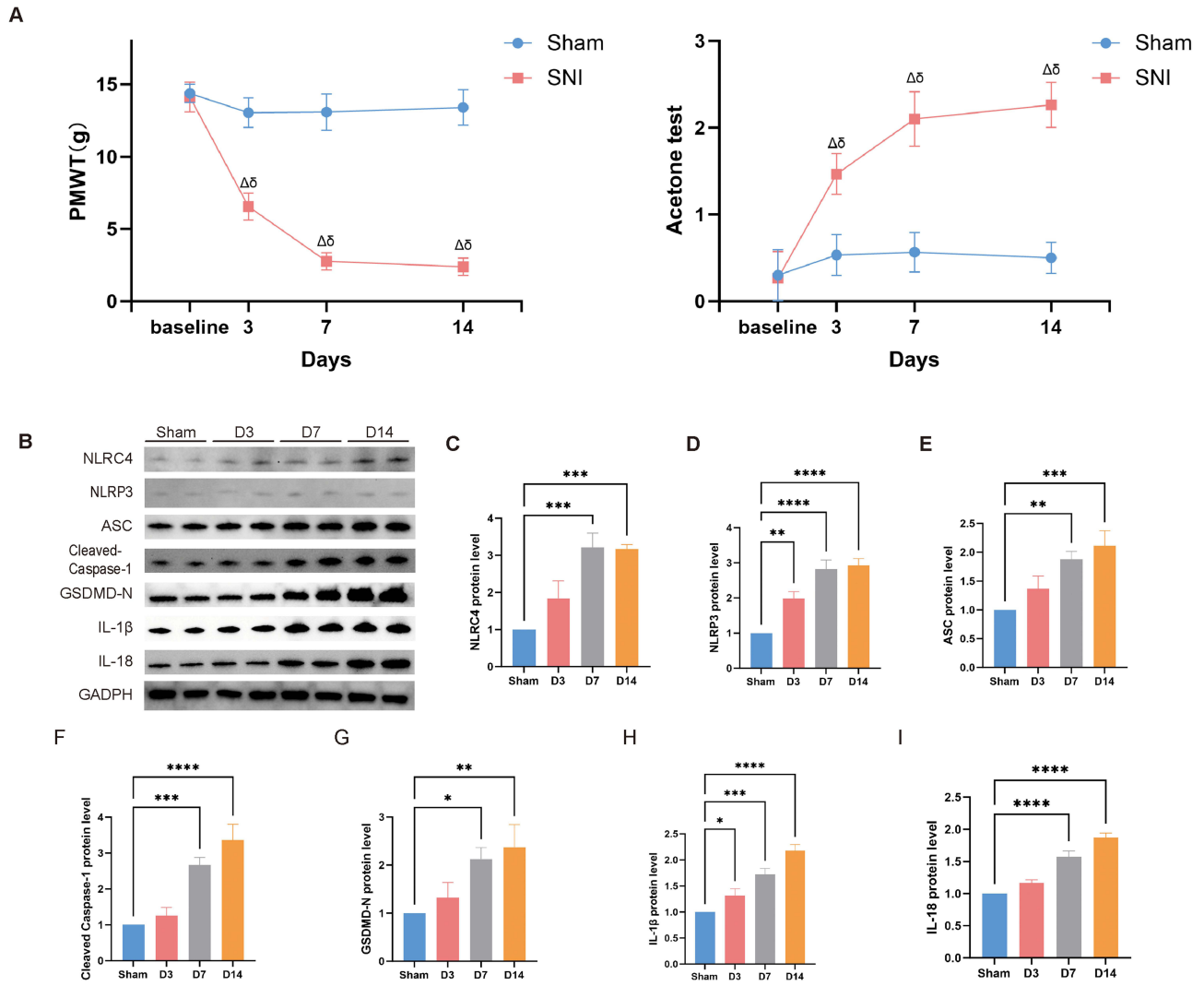

Figure 4 PMWT and NLRP3/NLRC4 inflammasomes activation in the spinal cord of the Sham and SNI group. (**A**) The PMWT test and Acetone Test (n=10); (**B**) the levels of NLRP3 and NLRC4 inflammasomes and their downstream proteins were significantly elevated in the spinal cord of SNI rats, correlating with the progression of the model (n=3); (**C**) Quantification of NLRC4 Western blotting data; (**D**) Quantification of NLRP3 Western blotting data; (**E**) Quantification of ASC Western blotting data; (**F**) Quantification of Cleaved-Caspase-1 Western blotting data; (**G**) Quantification of GSDMD-N Western blotting data; (**H**) Quantification of IL-1β Western blotting data; (**I**) Quantification of IL-18 Western blotting data. All data are presented as mean ± SEM. $^{\Delta}p < 0.05$, compared with the baseline. $^{\delta}p < 0.05$, compared with the Sham group. *p < 0.05, **p < 0.01, ***p < 0.001, ****p < 0.0001, compared with the Sham group.

18.[29,30] Each inflammasome complex typically consists of three main components: an upstream sensor molecule NLR protein, an adaptor protein ASC with PYD and CARD domains which links to the downstream effector protein caspase family. Among these, NLRP3 inflammasome-mediated pyroptosis has been the most extensively studied. Recent studies have found that NLRP3 inflammasome-mediated pyroptosis is elevated in the spinal cords of CCI rats, and that inhibiting pyroptosis can mitigate CCI-induced mechanical and thermal hyperalgesia.[31–33] Sun et al[34] found that modulating the NLRP3 inflammasome and pyroptosis in the dorsal root ganglion of diabetic rats can alleviate diabetic neuropathic pain. Wang et al[35] discovered that melatonin can suppress pyroptosis via the NF-κB/NLRP3 inflammasome signaling pathway in the SNL model, thereby exerting analgesic and anti-inflammatory effects. NLRC4 is also an NLR protein; Naip recognizes the flagellin protein and induces NLRC4 inflammasome activation, leading to pyroptosis.[36] However, only one study has confirmed that the mRNA expression level of spinal NLRC4 is significantly elevated in both male and female CCI rats.[37] NLRC4 differs in structure from NLRP3 which interact indirectly with caspase-1 via the PYD motif of the adaptor protein ASC, while NLRC4 lack the PYD motif, but contain a CARD motif, and so can interact directly with caspase-1, which also contains CARD, without the use of ASC adaptor.[37] These two common inflammasomes differ

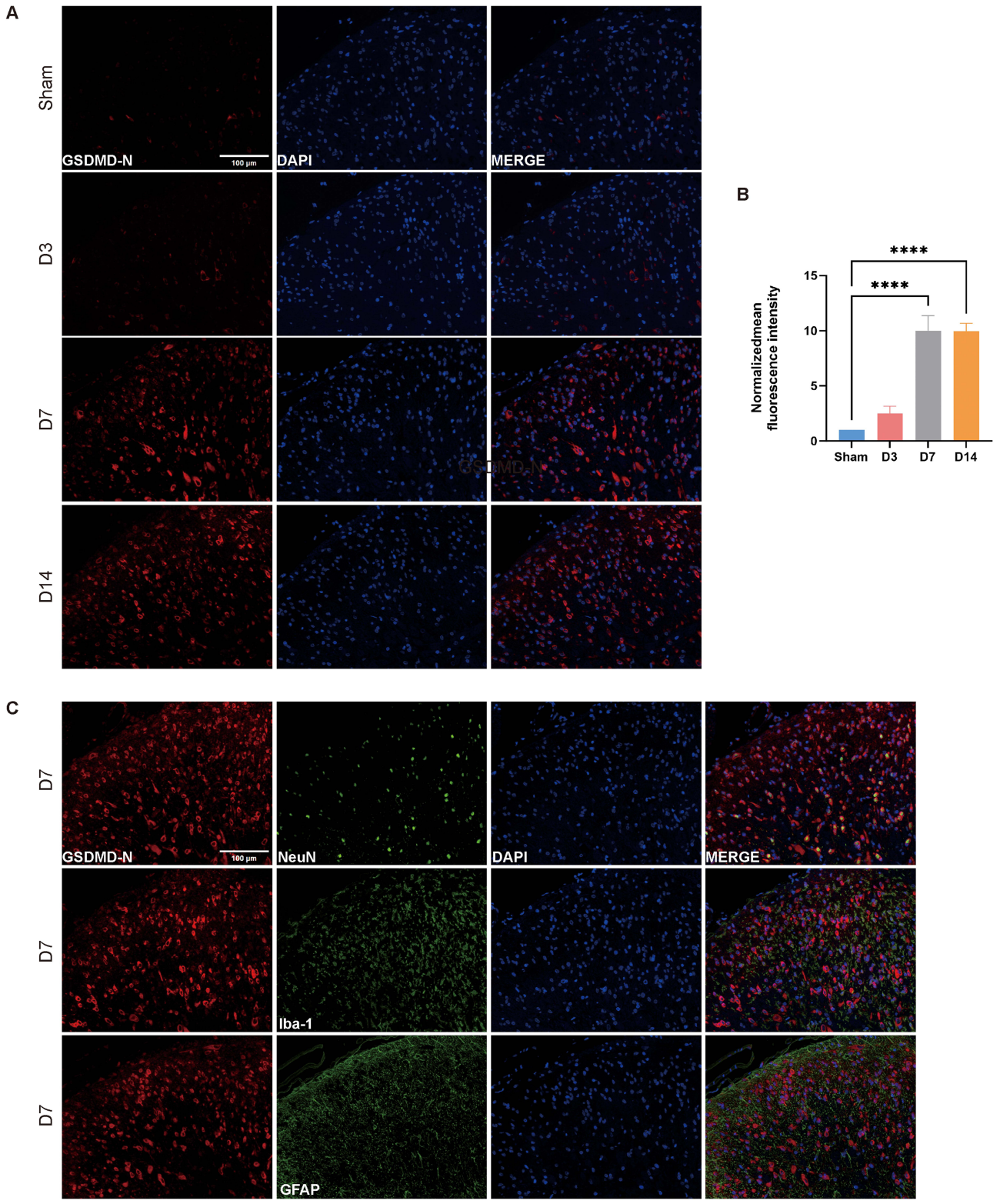

Figure 5 Cellular localization of pyroptosis in the spinal cord of the Sham and SNI group. (**A**) Immunofluorescence for GSDMD-N in the spinal cord (scale bar= 100μm); (**B**) Fluorescence intensity for GSDMD-N (n=3); (**C**) Double immunostaining for GSDMD-N and NeuN, Iba-1, and GFAP in the rat D7 after SNI (scale bar= 100μm). All data are presented as mean ± SEM. ****$p < 0.0001$, compared with the Sham group.

https://doi.org/10.2147/JPR.S568630

slightly in their structure and methods of activation, the shared ability of both inflammasomes to activate caspase-1, then trigger pyroptosis and release of IL-1β and IL-18 suggests a potential mechanism for their functional synergy.

Triggering receptor expressed on myeloid cells 2 (TREM2) is a cell surface receptor predominantly found on microglia within the central nervous system. In the SNI model, TREM2 signaling enhances the pro-inflammatory response of microglia and exacerbates neuropathic pain. Resveratrol administration can downregulate TREM2, reduce neuroinflammation, and improve hyperalgesia.[38,39] Interferon-induced protein Z-DNA binding protein 1 (ZBP1) is a crucial innate immune sensor. Upon detection of Z-RNA, ZBP1 recruits RIPK3 and caspase-8 to activate the ZBP1-NLRP3 inflammasome, inducing cell panoptosis.[40,41] However, the role of ZBP1 in NP remains to be fully elucidated.

GO enrichment analysis results demonstrate a primary association with immune response and inflammasomes. Both KEGG and GSEA results revealed that the NOD-like receptor signaling pathway is associated with NP. Recent research by Green-Fulgham et al[37] investigated changes in four inflammasomes (NLRP3, AIM2, NLRP1, and NLRC4) within the spinal cord of the CCI model. They found that CCI upregulated all four inflammasomes in both sexes, but there were sex differences in the relative levels of inflammasome expression. NLRP3 and AIM2 exhibit higher expression levels in females, while NLRP1 is expressed at higher levels in males. Among various inflammasomes, the NLRP3 inflammasome is the most extensively studied in NP research. After sciatic nerve injury in mice, the NLRP3 inflammasome is activated, resulting in the upregulation of inflammasome-related components and the release of IL-1β and IL-18. Moreover, NLRP3 knockout mice display a reduced inflammatory response and an increased sciatic functional index (SFI) following sciatic nerve injury.[42] In diabetic neuropathy, TXNIP is upregulated and binds to NLRP3, resulting in increased TXNIP-NLRP3 complex formation that induces IL-1β release and subsequent inflammation.[43]

IL-1β and IL-18 are released through membrane pores during pyroptosis, thereby amplifying the inflammatory response and activating immune reactions.[44,45] Conversely, IL-1ra is a natural anti-inflammatory antagonist within the pro-inflammatory cytokine interleukin-1 family.[46] Previous studies have confirmed that IL-1β levels in the spinal cords of rats significantly increase post-CCI, and administration of IL-1ra reduces NP symptoms and enhances the analgesic effects of morphine and buprenorphine in these rats.[47] He et al[48] found that the administration of IL-1ra to block IL-1β can reduce hyperalgesia in a nitroglycerin-induced chronic migraine model. A meta-analysis of cytokine levels in the bodily fluids of PHN patients showed that IL-1β levels in PHN patients were significantly elevated compared to the control group.[49] Compelling evidence indicates that IL-18 is upregulated in the development of chronic pain. Antagonizing or inhibiting IL-18 expression can mitigate the onset and progression of chronic pain.[50] Miyoshi et al[51] found that IL-18 and IL-18r expression in the dorsal horn of the spinal cord significantly increased in the SNL model. IL-18 and IL-18r were upregulated in activated microglia and astrocytes, respectively. Inhibiting the function of the IL-18 signaling pathway can alleviate pathological pain, while intrathecal injection of IL-18 can induce pathological pain.

Emerging evidence highlighting its roles across distinct cell types pyroptosis during NP pathogenesis. While most studies have focused on microglial pyroptosis between NP interactions, recent advances reveal broader cellular involvement. For example, Wu et al demonstrated that inhibiting the 7A-containing C-type lectin structural domain alleviates NP by modulating NLRP3 inflammasome-mediated microglial pyroptosis and attenuating neuroinflammation in both CCI rat models and LPS/ATP-treated BV2 microglial cells.[31] Similarly, the miR-99b-3p/Mmp13 axis exerts analgesic effects in CCI rats through NLRP3 suppression and autophagy promotion.[32] Schwann cell pyroptosis has also been implicated: Liu et al reported that Nrf2/HO-1 pathway activation in a trigeminal neuralgia model induces demyelination via Schwann cell pyroptosis.[52] Additionally, Chen et al showed that lysine acetyltransferase 2A-mediated p38 pathway succinylation drives chemotherapy-induced neuropathic pain (CINP) by promoting microglial pyroptosis.[53] Notably, two SNI model studies align with our findings. Chen et al found that botulinum toxin type A inhibits microglial pyroptosis in LPS-treated microglia and SNI rats, reducing NP.[54] Similarly, Li et al demonstrated that the translocator protein (TSPO) attenuates NP in SNI mice and LPS-treated astrocytes by blocking astrocytic pyroptosis via the AMPK-PGC-1α pathway.[55] In contrast, our immunofluorescence data revealed that GSDMD-N (a pyroptosis executioner protein) predominantly colocalizes with neurons-not microglia or astrocytes-in the spinal cord dorsal horn of SNI rats. This discrepancy may arise from differences between in vivo SNI pathology and in vitro LPS-stimulated models. Consistent with our results, Zhang et al[56] also observed pyroptosis exclusively in neurons within the spinal cord of SNI mice. In contrast, Deng et al[57] reported that GSDMD was co-localized with both neuronal and microglial markers in the spinal cord of SNI mice.

However, it is important to note that GSDMD does not acquire its pyroptosis-inducing biological function until it is cleaved into its N-terminal fragment (GSDMD-N). Therefore, the observed co-localization in microglia may not necessarily indicate the occurrence of pyroptosis in these cells. Collectively, our findings underscore neuronal pyroptosis as a critical mechanism in NP development, offering novel cellular insights specific to SNI models.

This study has several limitations. First, due to the variety and inconsistencies in characteristics of NP models, this study only used samples from the SNI model, which may be insufficient. Future studies should include clinical trials in patient populations to validate the translational potential of these findings. Second, the PRGs were obtained from literature or databases, meaning they are genes that have been experimentally verified, although there may still be undiscovered PRGs. Therefore, the PRGs identified in this study may be incomplete. Finally, it should be noted that this study was primarily based on bioinformatic analyses and preliminary experimental validation. Therefore, it is necessary to further investigate the roles of the NLRC4 and NLRP3 inflammasomes in NP and the potential mechanism of interaction between them.

Conclusion

In conclusion, We identified 11 potential biomarkers for NP. Our data conclusively show that SNI induced NLRP3/NLRC4 inflammasome activation and neuronal pyroptosis in the rat spinal cord.

Data Sharing Statement

The data of this study are available from the Rongguo Liu upon reasonable request.

Acknowledgments

The authors would like to thank all the colleagues who contributed to this work.

Funding

This work was sponsored by Joint Funds for Innovation of Science and Technology, Fujian Province (No. 2024Y9165), Joint Funds for Innovation of Science and Technology, Fujian Province (No. 2024Y9133) and Fujian Province Finance Project (No. BPB-2024LRG).

Disclosure

The authors declare that the research was conducted in the absence of any commercial or financial relationships that could be construed as a potential conflict of interest.

References

1. Jensen TS, Baron R, Haanpaa M, et al. A new definition of neuropathic pain. *Pain*. 2011;152(10):2204–2205. doi:10.1016/j.pain.2011.06.017
2. Scholz J, Finnerup NB, Attal N, et al. The IASP classification of chronic pain for ICD-11: chronic neuropathic pain. *Pain*. 2019;160(1):53–59. doi:10.1097/j.pain.0000000000001365
3. Thouaye M, Yalcin I. Neuropathic pain: from actual pharmacological treatments to new therapeutic horizons. *Pharmacol Ther*. 2023;251:108546. doi:10.1016/j.pharmthera.2023.108546
4. Attal N, Bouhassira D, Colvin L. Advances and challenges in neuropathic pain: a narrative review and future directions. *Br J Anaesth*. 2023;131(1):79–92.
5. Fiore NT, Debs SR, Hayes JP, Duffy SS, Moalem-Taylor G. Pain-resolving immune mechanisms in neuropathic pain. *Nat Rev Neurol*. 2023;19(4):199–220. doi:10.1038/s41582-023-00777-3
6. Ellis A, Bennett DL. Neuroinflammation and the generation of neuropathic pain. *Br J Anaesth*. 2013;111(1):26–37. doi:10.1093/bja/aet128
7. Teixeira-Santos L, Albino-Teixeira A, Pinho D. Neuroinflammation, oxidative stress and their interplay in neuropathic pain: focus on specialized pro-resolving mediators and NADPH oxidase inhibitors as potential therapeutic strategies. *Pharmacol Res*. 2020;162:105280. doi:10.1016/j.phrs.2020.105280
8. Ji RR, Nackley A, Huh Y, Terrando N, Maixner W. Neuroinflammation and central sensitization in chronic and widespread pain. *Anesthesiology*. 2018;129(2):343–366. doi:10.1097/ALN.0000000000002130
9. Broz P, Pelegrin P, Shao F. The gasdermins, a protein family executing cell death and inflammation. *Nat Rev Immunol*. 2020;20(3):143–157. doi:10.1038/s41577-019-0228-2
10. Shi J, Zhao Y, Wang K, et al. Cleavage of GSDMD by inflammatory caspases determines pyroptotic cell death. *Nature*. 2015;526(7575):660–665. doi:10.1038/nature15514

11. Sborgi L, Ruhl S, Mulvihill E, et al. GSDMD membrane pore formation constitutes the mechanism of pyroptotic cell death. *EMBO J*. 2016;35 (16):1766–1778. doi:10.15252/embj.201694696
12. Li B, Guo J, Zhou X, et al. The emerging role of pyroptosis in neuropathic pain. *Int Immunopharmacol*. 2023;121:110562. doi:10.1016/j.intimp.2023.110562
13. Ghazisaeidi S, Muley MM, Tu Y, et al. Conserved transcriptional programming across sex and species after peripheral nerve injury predicts treatments for neuropathic pain. *Br J Pharmacol*. 2023;180(21):2822–2836. doi:10.1111/bph.16168
14. Howe K, Dwinell M, Shimoyama M, et al. The genome sequence of the Norway rat, Rattus norvegicus Berkenhout 1769. *Wellcome Open Res*. 2021;6:118. doi:10.12688/wellcomeopenres.16854.1
15. de Jong TV, Pan Y, Rastas P, et al. A revamped rat reference genome improves the discovery of genetic diversity in laboratory rats. *Cell Genom*. 2024;4(4):100527. doi:10.1016/j.xgen.2024.100527
16. Yan M, Li W, Wei R, et al. Identification of pyroptosis-related genes and potential drugs in diabetic nephropathy. *J Transl Med*. 2023;21(1):490. doi:10.1186/s12967-023-04350-w
17. Aleksander SA, Balhoff J, Carbon S, et al. The gene ontology knowledgebase in 2023. *Genetics*. 2023;224(1). doi:10.1093/genetics/iyad031
18. Liberzon A, Subramanian A, Pinchback R, et al. Molecular signatures database (MSigDB) 3.0. *Bioinformatics*. 2011;27(12):1739–1740. doi:10.1093/bioinformatics/btr260
19. Zhou G, Soufan O, Ewald J, et al. NetworkAnalyst 3.0: a visual analytics platform for comprehensive gene expression profiling and meta-analysis. *Nucleic Acids Res*. 2019;47(W1):W234–W241. doi:10.1093/nar/gkz240
20. Yu G, Wang LG, Han Y, He QY. clusterProfiler: an R package for comparing biological themes among gene clusters. *OMICS*. 2012;16(5):284–287. doi:10.1089/omi.2011.0118
21. Subramanian A, Tamayo P, Mootha VK, et al. Gene set enrichment analysis: a knowledge-based approach for interpreting genome-wide expression profiles. *Proc Natl Acad Sci USA*. 2005;102(43):15545–15550. doi:10.1073/pnas.0506580102
22. Szklarczyk D, Kirsch R, Koutrouli M, et al. The STRING database in 2023: protein–protein association networks and functional enrichment analyses for any sequenced genome of interest. *Nucleic Acids Res*. 2023;51(D1):D638–D646. doi:10.1093/nar/gkac1000
23. Decosterd I, Woolf CJ. Spared nerve injury: an animal model of persistent peripheral neuropathic pain. *Pain*. 2000;87(2):149–158. doi:10.1016/S0304-3959(00)00276-1
24. Dixon WJ. Efficient analysis of experimental observations. *Annu Rev Pharmacol Toxicol*. 1980;20(1):441–462. doi:10.1146/annurev.pa.20.040180.002301
25. Bouhassira D. Neuropathic pain: definition, assessment and epidemiology. *Rev Neurol*. 2019;175(1–2):16–25. doi:10.1016/j.neurol.2018.09.016
26. Finnerup NB, Kuner R, Jensen TS. Neuropathic pain: from mechanisms to treatment. *Physiol Rev*. 2021;101(1):259–301. doi:10.1152/physrev.00045.2019
27. Colloca L, Ludman T, Bouhassira D, et al. Neuropathic pain. *Nat Rev Dis Primers*. 2017;3(1):17002. doi:10.1038/nrdp.2017.2
28. Wang X, Peng M, Weng L, et al. Bibliometric study of the comorbidity of pain and depression research. *Neural Plast*. 2019;2019:1657498. doi:10.1155/2019/1657498
29. Liu X, Zhang Z, Ruan J, et al. Inflammasome-activated gasdermin D causes pyroptosis by forming membrane pores. *Nature*. 2016;535 (7610):153–158. doi:10.1038/nature18629
30. Yao J, Sterling K, Wang Z, Zhang Y, Song W. The role of inflammasomes in human diseases and their potential as therapeutic targets. *Signal Transduct Target Ther*. 2024;9(1):10. doi:10.1038/s41392-023-01687-y
31. Wu D, Zhang Y, Zhao C, et al. Disruption of C/EBPbeta-Clec7a axis exacerbates neuroinflammatory injury via NLRP3 inflammasome-mediated pyroptosis in experimental neuropathic pain. *J Transl Med*. 2022;20(1):583. doi:10.1186/s12967-022-03779-9
32. Gao X, Gao LF, Zhang ZY, Jia S, Meng CY. miR-99b-3p/Mmp13 axis regulates NLRP3 inflammasome-dependent microglial pyroptosis and alleviates neuropathic pain via the promotion of autophagy. *Int Immunopharmacol*. 2024;126:111331. doi:10.1016/j.intimp.2023.111331
33. Wu D, Wang P, Zhao C, et al. Levo-tetrahydropalmatine ameliorates neuropathic pain by inhibiting the activation of the Clec7a-MAPK/NF-kappaB -NLRP3 inflammasome axis. *Phytomedicine*. 2023;121:155075. doi:10.1016/j.phymed.2023.155075
34. Sun Q, Zhang R, Xue X, et al. Jinmaitong alleviates diabetic neuropathic pain through modulation of NLRP3 inflammasome and gasdermin D in dorsal root ganglia of diabetic rats. *Front Pharmacol*. 2021;12:679188. doi:10.3389/fphar.2021.679188
35. Wang Y, Gao X, Tang Y, et al. The role of NF-kappaB/nlrp3 inflammasome signaling pathway in attenuating pyroptosis by melatonin upon spinal nerve ligation models. *Neurochem Res*. 2022;47(2):335–346. doi:10.1007/s11064-021-03450-7
36. Duncan JA, Canna SW. The NLRC4 Inflammasome. *Immunol Rev*. 2018;281(1):115–123. doi:10.1111/imr.12607
37. Green-Fulgham SM, Ball JB, Kwilasz AJ, et al. Interleukin-1beta and inflammasome expression in spinal cord following chronic constriction injury in male and female rats. *Brain Behav Immun*. 2024;115:157–168. doi:10.1016/j.bbi.2023.10.004
38. Kobayashi M, Konishi H, Sayo A, Takai T, Kiyama H. TREM2/DAP12 signal elicits proinflammatory response in microglia and exacerbates neuropathic pain. *J Neurosci*. 2016;36(43):11138–11150. doi:10.1523/JNEUROSCI.1238-16.2016
39. Wang Y, Shi Y, Huang Y, et al. Resveratrol mediates mechanical allodynia through modulating inflammatory response via the TREM2-autophagy axis in SNI rat model. *J Neuroinflammation*. 2020;17(1):311. doi:10.1186/s12974-020-01991-2
40. Zheng M, Kanneganti T. The regulation of the ZBP1-NLRP3 inflammasome and its implications in pyroptosis, apoptosis, and necroptosis (PANoptosis). *Immunol Rev*. 2020;297(1):26–38. doi:10.1111/imr.12909
41. Kuriakose T, Man SM, Malireddi RKS, et al. ZBP1/DAI is an innate sensor of influenza virus triggering the NLRP3 inflammasome and programmed cell death pathways. *Sci Immunol*. 2016;1(2). doi:10.1126/sciimmunol.aag2045
42. Cui M, Liang J, Xu D, et al. NLRP3 inflammasome is involved in nerve recovery after sciatic nerve injury. *Int Immunopharmacol*. 2020;84:106492. doi:10.1016/j.intimp.2020.106492
43. Xu L, Lin X, Guan M, Zeng Y, Liu Y. Verapamil attenuated prediabetic neuropathy in high-fat diet-fed mice through inhibiting TXNIP-mediated apoptosis and inflammation. *Oxid Med Cell Longev*. 2019;2019:1896041. doi:10.1155/2019/1896041
44. Fink SL, Cookson BT. Pyroptosis and host cell death responses during Salmonella infection. *Cell Microbiol*. 2007;9(11):2562–2570. doi:10.1111/j.1462-5822.2007.01036.x
45. Fink SL, Cookson BT. Caspase-1-dependent pore formation during pyroptosis leads to osmotic lysis of infected host macrophages. *Cell Microbiol*. 2006;8(11):1812–1825. doi:10.1111/j.1462-5822.2006.00751.x

46. Akash MSH, Rehman K, Chen S. IL-1Ra and its delivery strategies: inserting the association in perspective. *Pharm Res*. 2013;30(11):2951–2966. doi:10.1007/s11095-013-1118-0
47. Pilat D, Rojewska E, Jurga AM, et al. IL-1 receptor antagonist improves morphine and buprenorphine efficacy in a rat neuropathic pain model. *Eur J Pharmacol*. 2015;764:240–248. doi:10.1016/j.ejphar.2015.05.058
48. He W, Long T, Pan Q, et al. Microglial NLRP3 inflammasome activation mediates IL-1beta release and contributes to central sensitization in a recurrent nitroglycerin-induced migraine model. *J Neuroinflammation*. 2019;16(1):78. doi:10.1186/s12974-019-1459-7
49. Yue J, Yao M. Humoral cytokine levels in patients with herpes zoster: a meta-analysis. *J Pain Res*. 2024;17:887–902. doi:10.2147/JPR.S449211
50. Ju J, Li Z, Jia X, et al. Interleukin-18 in chronic pain: focus on pathogenic mechanisms and potential therapeutic targets. *Pharmacol Res*. 2024;201:107089. doi:10.1016/j.phrs.2024.107089
51. Miyoshi K, Obata K, Kondo T, Okamura H, Noguchi K. Interleukin-18-mediated microglia/astrocyte interaction in the spinal cord enhances neuropathic pain processing after nerve injury. *J Neurosci*. 2008;28(48):12775–12787. doi:10.1523/JNEUROSCI.3512-08.2008
52. Liu M, Wang Y, Li S, et al. Attenuates reactive oxygen species: induced pyroptosis via activation of the Nrf2/HO-1 signal pathway in models of trigeminal neuralgia. *Sci Rep*. 2023;13(1):18111. doi:10.1038/s41598-023-44013-w
53. Chen R, Hu J, Zhang Y, et al. Total glucosides of paeony ameliorates chemotherapy-induced neuropathic pain by suppressing microglia pyroptosis through the inhibition of KAT2A-mediated p38 pathway activation and succinylation. *Sci Rep*. 2024;14(1):31875. doi:10.1038/s41598-024-83207-8
54. Chen LP, Gui XD, Tian WD, et al. Botulinum toxin type A-targeted SPP1 contributes to neuropathic pain by the activation of microglia pyroptosis. *World J Psychiatry*. 2024;14(8):1254–1266. doi:10.5498/wjp.v14.i8.1254
55. Li B, Yu K, Zhou X, et al. Increased TSPO alleviates neuropathic pain by preventing pyroptosis via the AMPK-PGC-1alpha pathway. *J Headache Pain*. 2025;26(1):16. doi:10.1186/s10194-025-01953-0
56. Zhang X, Miao Y, Li Z, Xu H, Niu Z. ACVR1 drives neuropathic pain by regulating NLRP3-Induced neuronal pyroptosis through the p38 and Smad1/5/8 pathways. *Neuropharmacology*. 2025;274:110469. doi:10.1016/j.neuropharm.2025.110469
57. Deng D, Ma L, Shen J, et al. PD-1 attenuates neuropathic pain by ameliorating NLRP3 inflammasome-mediated microglia pyroptosis. *Mol Neurobiol*. 2025;62(12):15478–15493. doi:10.1007/s12035-025-05225-5